Paper No.
10379

NACE INTERNATIONAL CORROSION 2010 CONFERENCE & EXPO

Internal CO_2 Corrosion of Mild Steel Pipelines under Inert Solid Deposits

Jin Huang, Bruce Brown, Xiu Jiang, Brian Kinsella and Srdjan Nesic[1]
Institute for Corrosion and Multiphase Technology, Ohio University
342 west state street, Athens, OH, 45701

Under-deposit CO_2 corrosion occurs when solids like sand, corrosion products, wax or a variety of other particles deposit on the bottom of pipelines, forming a bed or layer of solids[1,2]. Under-deposit CO_2 corrosion is different from "regular" CO_2 corrosion as the aqueous solution beneath the solids is chemically and physically different from the "bulk" solution in the pipe. The presence of solids can also limit inhibitor access to the metal surface which can initiate severe localized corrosion [3].

Initial testing was directed towards defining and modeling the fundamental mild steel CO_2 corrosion mechanisms occurring in the presence of clean inert solid deposits with different particle sizes and shapes (SiO_2 powder, glass beads (GB) and sand). Experiments were conducted in a glass cell at a total pressure of 1 bar for temperatures of 25°C and 80°C. The mild steel sample was immersed in 1 wt% NaCl electrolyte for one day. Corrosion behavior was characterized by electrochemical techniques, including LPR (linear polarization resistance), EIS (electrochemical impedance spectroscopy) and potentiodynamic sweeps. Steel surface morphologies have been analyzed by using SEM (scanning electron microscope) and EDX (energy dispersive x-ray).

Keywords: solids, under-deposit, CO_2 corrosion, mild steel, pipelines

[1] Corresponding author email address: nesic@ohio.edu (S. Nesic)

INTRODUCTION

Severe corrosion problems such as crevice corrosion and pitting can be found under solid deposits in pipelines [2]. Localized corrosion occurs under these deposits because they provide a region that is chemically and physically different from the rest of the steel surface which is not covered [4]. This difference may generate a galvanic corrosion cell or affect inhibitor performance or provide ideal conditions for bacterial growth [3]. Under-deposit corrosion is prevalent at the bottom of horizontal lines where flow rates are not large enough to keep the solids suspended. However, no work is reported in the open literature that covers the mechanisms of under-deposit corrosion as most of literature refers to the effect of deposits on inhibitor performance[4,5,6]. Pedersen, et al.[5] developed a test method for studying under-deposit corrosion and investigated the inhibitor performance under sand deposits. Their work, while being useful in many ways, does not focus on the mechanism of the corrosion process under the deposit.

The goal of this work is to gain an initial understanding of the CO_2 corrosion mechanism of mild steel covered by inert deposits by experimentally studying the effects of deposit porosity, deposit thickness, solution pH, and temperature and by deploying the in-situ electrochemical and techniques. The effect of the deposits on inhibitor performances and potential galvanic effects related to under-deposit corrosion were not covered in this stage of the project.

EXPERIMENTAL PROCEDURE

All tests were conducted in a glass cell using a standard three-electrode set up, as shown in Figure 1. The glass cell was filled with 2 liters of DI water with 1%wt NaCl . X65 mild steel was used as the working electrode (WE) for electrochemical measurements. Platinum wire was used as a counter electrode (CE) and a saturated silver-silver chloride (Ag/AgCl) electrode was used as a reference electrode (RE).

Electrochemical techniques including linear polarization resistance (LPR), potentiodynamic sweeps (PDS) and electrochemical impedance spectroscopy (EIS) were used to measure the corrosion rate and identify the corrosion mechanisms of mild steel both with and without solid deposits. The WE was polarized ±5mV from open circuit potential (E_{oc}) during the LPR measurements at a scan rate of 0.125mV/s to obtain the polarization resistance R_p, which was then used to calculate the general corrosion rate of mild steel. For the EIS measurement, a sinusoidal potential signal ±5mV peak-to-peak around E_{oc} was applied to the WE, scanning from 10kHz to 1mHz. This scan enables the identification of both the solution resistance (R_s) – at the highest frequency range and the "fingerprint" of the various reactions involved in the corrosion process – at the lower frequency ranges. Corrosion mechanisms were also studied by using

potentiodynamic sweeps which were conducted in two steps. Polarization of the WE started from E_{oc} by sweeping the potential at a scan rate of 0.125mV/s in the cathodic (more negative) direction by 0.4V, and then disconnecting and pausing until stable E_{oc} was attained again, when the potential of the WE was swept in the anodic (more positive) direction by 0.2V using the same scan rate.

Conditions for the under-deposit corrosion experiments are summarized in the test matrix outlined in Table 1. Before being immersed into the electrolyte, the WE surface was polished by using 200, 400 and 600 grit silica carbide (SiC) paper wetted with water, then rinsed with isopropanol, and air dried. The electrolyte in the glass cell was purged continuously with CO_2 during each test to maintain the CO_2 partial pressure and remove dissolved oxygen. Separate measurements have proven that this experimental setup/procedure ensures that the concentration of dissolved oxygen does not exceed 20 ppb what is considered acceptable.

Baseline experiments included corrosion measurements on "bare" mild steel and under-deposit corrosion tests as outlined the test matrix shown in Table 1. Before each under-deposit experiment, the steel sample was immersed in the electrolyte for about one hour without a deposit, where the bare corrosion rate and solution resistance were measured by LPR and EIS, to ensure that similar initial surface conditions were achieved before each experiment. Then the deposit was introduced and test was carried out for a further 24 hours.

Corroded steel surface morphologies and composition have been analyzed by using SEM and EDX. Surface pH measurements were also conducted by using a specially designed surface pH probe[7], which confirmed that a different pH is found under the solid deposit layer.

Testing sample holder

All corrosion samples were cylindrical, made from X65 mild steel, with a surface area of 8 cm^2 (0.0008 m^2) and height of 6.35 mm. The samples were mounted in a specially designed sample holder, where only the top surface of the steel sample was exposed to the environment with an O-ring separating the rest of the cylinder from the corrosive environment. At the bottom surface of the steel sample, spring loaded gold contact pins are used for electrochemical connections. The cylindrical steel sample and the sample holder are shown in Figure 2.

Deposit properties

The deposit types used in this work were sand, powder and glass beads. All of these deposits are the same base material, i.e. silica dioxide SiO_2. The main difference between them is their grain size and shape, as can be seen in SEM images shown in Figure 3. The deposit porosity was experimentally determined. For each deposit, a specific amount of DI water V_{water} (ml) was

added to dry deposit V_s (ml), the total volume of deposit and DI water V_{total} was recorded and porosity then was calculated:

$$porosity = \frac{V_s + V_{water} - V_{total}}{V_s}$$

The different grain sizes result in different physical properties, which are listed in Table 2.

Deposit preparation

All deposits used in this work were cleaned by 1 M sodium hydroxide solution, 5 M HCl acid solution and DI water to remove possible impurities before being used. The deposit was submerged in a 1wt% NaCl solution and stored in a separate beaker purged by CO_2 to remove dissolved oxygen. The pH of the deposit-electrolyte solution was also adjusted by $NaHCO_3$ solution to the same pH as the testing electrolyte. After the test sample was pre-corroded for about one hour, the cleaned deposit was transferred by a Pipet to the glass cell.

RESULTS AND DISCUSSION

Effect of deposit porosity and deposit thickness

It is seen in Figure 4 that introducing a deposit on the steel surface caused a sudden decrease in the corrosion rate by a factor 2 to 4 and then remained stable for 24 hours. The first data point of each data set was recorded before the deposit was introduced which shows repeatability of the initial condition. The corrosion rate data indicates that the more porous the deposit, the more the steel corroded as would be expected. As a first approximation, a linear relationship between corrosion rate and deposit porosity was found, see Figure 5. The corresponding corrosion potential change was also recorded, as seen in Figure 6. As compared to a bare steel, the corrosion potential increased by about 10-20mV for different deposits. The potentiodynamic sweeps measurements done at the end of the test after 24 hours are, shown in Figure 7. It can be seen that both anodic and cathodic reactions were retarded by the presence of a solid deposit. Further experiments were conducted at 25°C, pH 5, by using sand deposit with different thicknesses. It was observed that the thicker the deposit, the smaller the corrosion rate (Figure 8**).** It is understandable that an increase in deposit density (i.e. decrease in deposit porosity) and/or increase in deposit thickness slows down the diffusion of corrosive species and the corrosion products, resulting in a smaller corrosion rate.

Effect of the temperature

Figure 9 shows the effect of different temperatures on corrosion rate of mild steel. A test using 5 mm SiO_2 layer was conducted at 80°C. The corrosion rate change for metal with and without

deposit at 80°C was similar to that obtained at 25°C. A sudden decrease in corrosion rate was observed after the deposit was introduced at both temperatures and remained constantly.

Effect of the solution pH

Tests were also conducted at different bulk solution pH to investigate the possible effect of solution pH on the corrosion of mild steel in the presence of solid deposit. However, no significant differences in corrosion rate at different solution pH were observed, see Figure 10. This is very different from what is observed in bare steel CO_2 corrosion[8], where changing the bulk pH directly affects the overall corrosion rate.

pH underneath the solid deposit

All the experimental results discussed above (effect of deposit porosity, deposit thickness, temperature and bulk solution pH) lead to the conclusion that the water chemistry "within" or "underneath" the deposit layer is different from the bulk solution and needs to be defined. A method to measure that change was needed and the pH was the first property considered. The surface pH measurement technique developed by Han[7] was used.

Figure 11 to Figure 14 show the comparison of surface pH with bulk pH at different test conditions. All tests were conducted at the conditions as outlined in Table 1. It can be seen that the pH measured of 6.25 ± 0.25 pH units is independent of deposit type, bulk pH, and temperature. This explains the observation that the bulk solution pH didn't affect the corrosion of mild steel in the presence of inert solid deposit (Figure 10).

Steel surface morphology analysis

Steel sample surfaces have been analyzed by means of SEM and EDX after each test. The deposits on the steel surfaces were removed by carefully rinsing with alcohol immediately after the test sample was taken out of the glass cell. The steel sample was then sent immediately to SEM for analysis. After one day at 25°C, no iron carbonate crystals were present on the steel surface (Figure 15). The morphology of the steel surface corroded under inert deposits at 25°C is similar to a bare steel surface. Only a few scattered iron carbonate crystals were observed on the steel surface after one day's immersion at 80°C, see Figure 16. Within only one day exposure time, no localized corrosion was found at the steel surface in the presence of solid deposits.

EIS measurements

EIS is an electrochemical method in which an external alternating current (AC) signal is applied to a corroding metal, and the response measured[9]. Alternating current measurements at different frequencies enable different processes to be identified and measured[10]. At the very least, EIS can be used to measure the solution resistance (R_s) and polarization resistance (R_p).

In this work, the EIS technique was used to study the mechanisms of CO_2 corrosion of mild steel in the presence of a solid inert deposit. Figure 17 shows Nyquist curves obtained from EIS measurement for tests conducted at solution pH 5 at 25°C with 5mm deposit over 24 hours. The corresponding LPR, corrosion potential and potentiodynamic sweep measurement results are shown in Figure 4, Figure 6 and Figure 7. Fromn the Nyquist curves, it can be seen that the more porous the deposit (Table 2), the smaller the solution resistance, but all measured R_s values are larger than the R_s value for bare steel. Moreover, there is a second arc appearing at low frequency range in the Nyquist plot when there is deposit present, where only one arc is present in bare steel corrosion. This difference suggests a difference in mechanisms of the corrosion process on the steel surface covered with deposit as compared to bare steel. The corresponding Bode plots (Figure 18) show one crest in the high frequency range, a peak in the middle frequency range and another crest in the low frequency range, where for bare steel, only one peak in the middle frequency range was observed. This difference in Bode plots also indicates a different mechanism of metal corrosion in the presence of deposit as compared with bare steel[10]. Figure 19 and Figure 20 show a similar behavior of mild steel corroding in the presence of 5 mm SiO_2 deposit at pH 5 for both 25°C and 80°C. The differences between bare steel corrosion and steel corrosion in the presence of solid deposits observed in Nyquist plots and Bode plots discussed above, suggest that there might be an intermediate adsorption process involved in the corrosion reactions due to the introduction of the inert solid deposit. This hypothesis will be tested in the next stage of this project.

With all the experimental observations discussion above, it is therefore concluded that the inert solid deposits provided a mass transfer barrier for corrosive species and indicated an enhanced importance of an intermediate adsorption process. Both effects led to reduction in the overall corrosion rate of mild steel.

However, this is not to suggest that inert solid deposits always lead to a CO_2 corrosion rate reduction for mild steel. For example in the presence of oxygen, serious corrosion is observed [2], apparently due to formation of galvanic cells. In the case of inhibition, it has been reported that inhibitor performance can be problematic underneath solid deposit [4]. Finally, solid deposits have always been associated with bacterial activity and localized corrosion. These aspects of under-deposit corrosion have not been covered yet in this project, and will be studied in the near future. The work presented above is to be considered as a foundation for studying the effect of these complication factors in under-deposit CO_2 corrosion of mild steel.

CONCLUSIONS

- General CO_2 corrosion rate of mild steel decreases significantly underneath inert solid deposit with both anodic and cathodic reactions retarded.
- A linear relationship was observed between the deposit porosity and corrosion rate.
- Bulk solution pH had no effect on CO_2 corrosion of mild steel in the presence of inert solid deposit.
- The pH under the deposit was significantly higher than the bulk solution pH.

ACKNOWLEDGEMENTS

The authors would like to thank the sponsor companies of the Corrosion Center Joint Industry Project, , including BP, Champion Technologies, Clariant, ConocoPhillips, Ionik Consulting, Eni, ExxonMobile, Nalco, Total, Saudi Aramco, Tenaris, BR Petrobras, Chevron, BG Group, Baker Petrolite,, PTTEP, Petronas, Encana, Oxy, Teikoku, for their financial support.

REFERENCES

1. S. Papavinasam, A. Doiron, R. W. Revie., "Empirical equations to predict conditions for solid deposition", Material Performance August 2007
2. T. R. Jack, "Biological corrosion failures", ASM Handbook Vol.11 Failure analysis and prevention (#06072G), 2002
3. D. H. Pope, T. P. Zintel, "Methods for investigating under-deposit microbiologically influenced corrosion-a review", Material Performance, November 1989
4. D. I. Horsup, J. C. Clark, Bernard, P. Binks, P. D. I. Fletcher and J. T. Hicks, "I put it in, but where does it go?- the fate of corrosion inhibitors in multiphase systems", NACE 2007, paper No. 07617
5. A. Pedersen, K. Bilkova, E. Gulbrandsen, J. Kvarekvål "CO_2 corrosion inhibitor performance in the presence of solids: test method development", NACE 2008, paper No. 08632
6. C. Cathrea and A. Shankardass, "Understanding the synergistic effects of corrosion inhibitors and surfactants on erosion-corrosion and under-deposit corrosion in low velocity oil and sand slurry transportation systems", Champion Technologies, 2007
7. J. Han, "Under-deposit surface pH measurement", Chapter 07, ICMT CCJIP Board Meeting Presentation, Nov. 2008, Athens, Ohio
8. S. Nesic, J. Postlethwaite and S. Olsen, "An electrochemical model for prediction of corrosion of mild steel in aqueous carbon dioxide solutions", Corrosion Science, Vol. 52, No. 4, 1996
9. R. Cottis, S. Turgoose, "Electrochemical Impedance and Noise, Corrosion Testing Made Easy", editor B. C. Syrett, NACE International, 1999
10. J. K. Lee, "A mechanistic modeling of CO_2 corrosion of mild steel in the presence of H_2S", Ohio University Thesis, 2004

TABLES

Table 1 Test Matrix

Parameter	Conditions
Steel type	X65 carbon steel
P_{total} (bar)	1
Temperature (°C)	25, 80
CO_2 partial pressure (bar)	0.96, 0.54
Electrolyte	1% wt NaCl
Solution pH	4, 5, 6
Deposit	Silica sand, SiO_2 powder, glass beads
Deposit thickness (mm)	0, 2, 5, 10
Test duration (hour)	24

Table 2 Measured deposit properties

	Grain size	Bulk density*	Porosity#
SiO_2 powder	44 μm	0.75 g/cm^3	75%
sand	240 μm	2.5 g/cm^3	39%
glass beads	60 μm	2.5 g/cm^3	33%

* The mass of many particles of the material divided by the total volume they occupy.

The percentage of the volume of voids in a material composed of particles to the total volume the particles occupy.

FIGURES

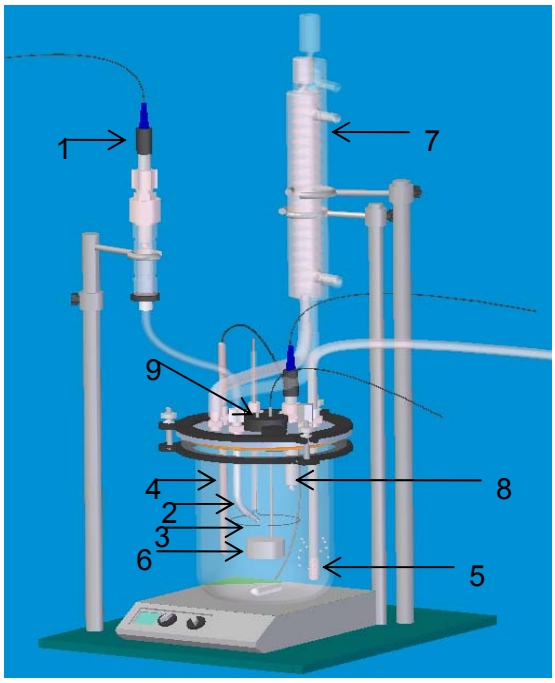

1. Reference Electrode
2. Luggin capillary
3. Platinum Counter Electrode
4. Temperature Probe
5. Bubbler
6. Working Electrode (X65 carbon steel)
7. Condenser
8. pH meter
9. Deposit Inlet

Figure 1 Standard three electrode glass cell set up for under-deposit CO_2 corrosion tests

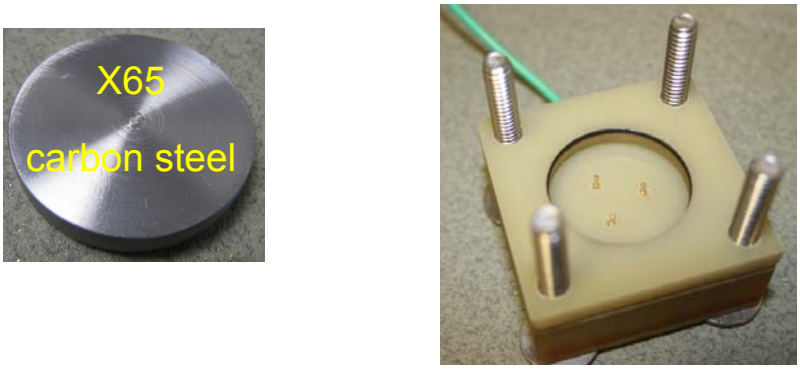

Figure 2 Steel sample and sample holder

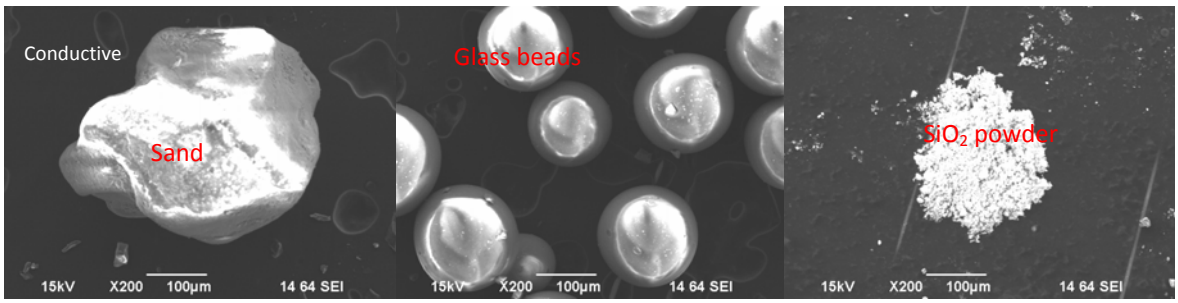

Figure 3 SEM images of deposit particles

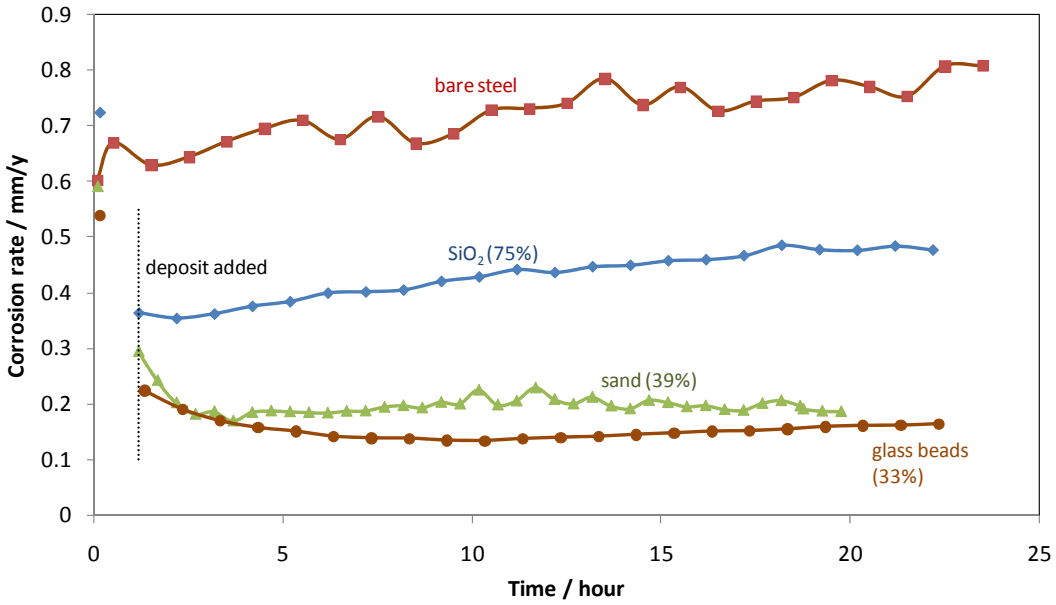

Figure 4 CO_2 corrosion rate of mild steel calculated from LPR measurements in the presence of a 5mm layer of different deposits at pH 5 and 25°C. Bare steel corrosion rate is 0.75 mm/y.

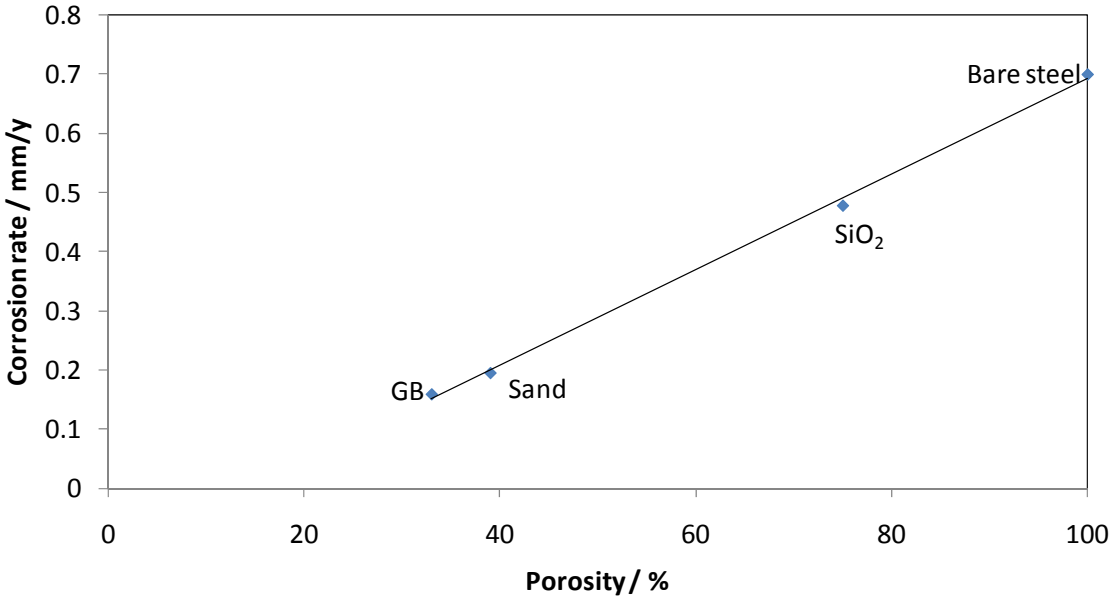

Figure 5 Linear relationships between deposit porosity and CO_2 corrosion rate.

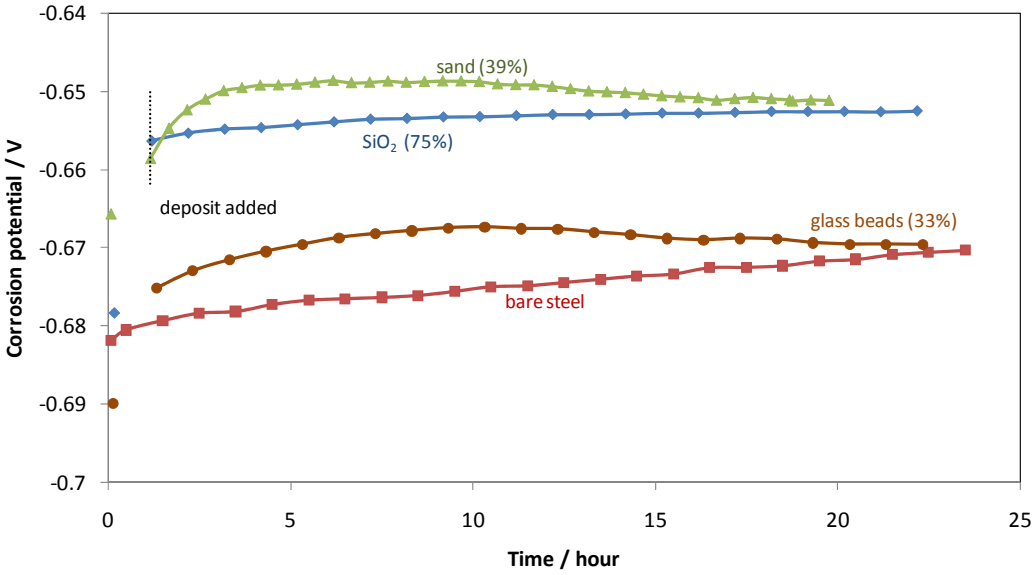

Figure 6 Corrosion potential of mild steel or tests conducted at pH 5 and 25°C in the presence of a 5mm deposit.

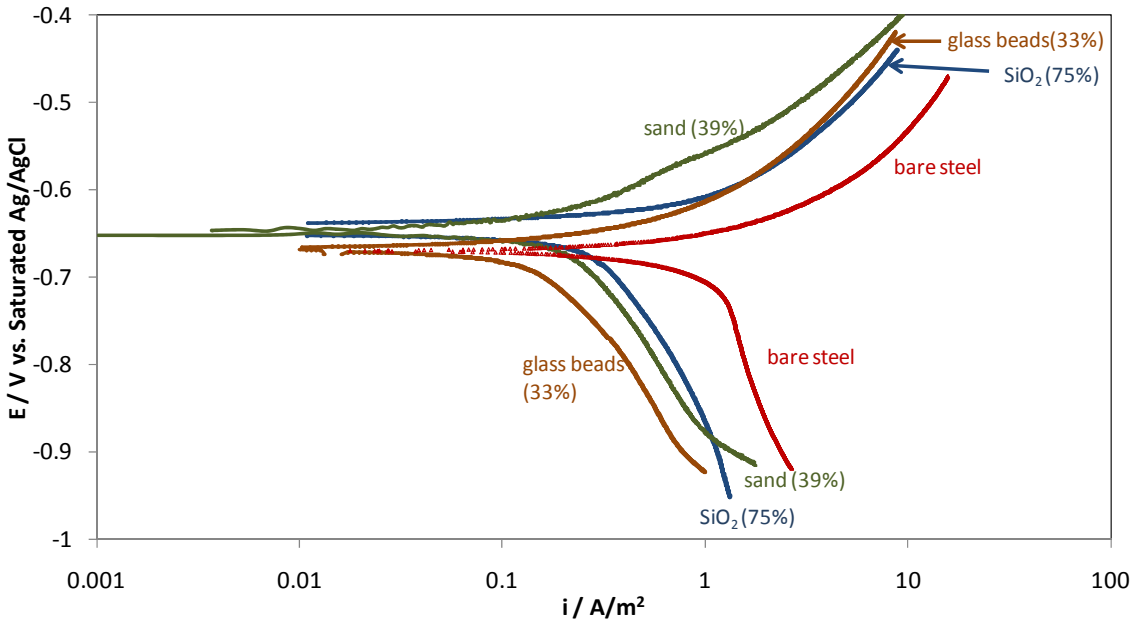

Figure 7 Potentiodynamic sweeps in mild steel CO_2 corrosion in the presence of a 5mm layer of different deposits at pH 5 and 25°C after 24 hours.

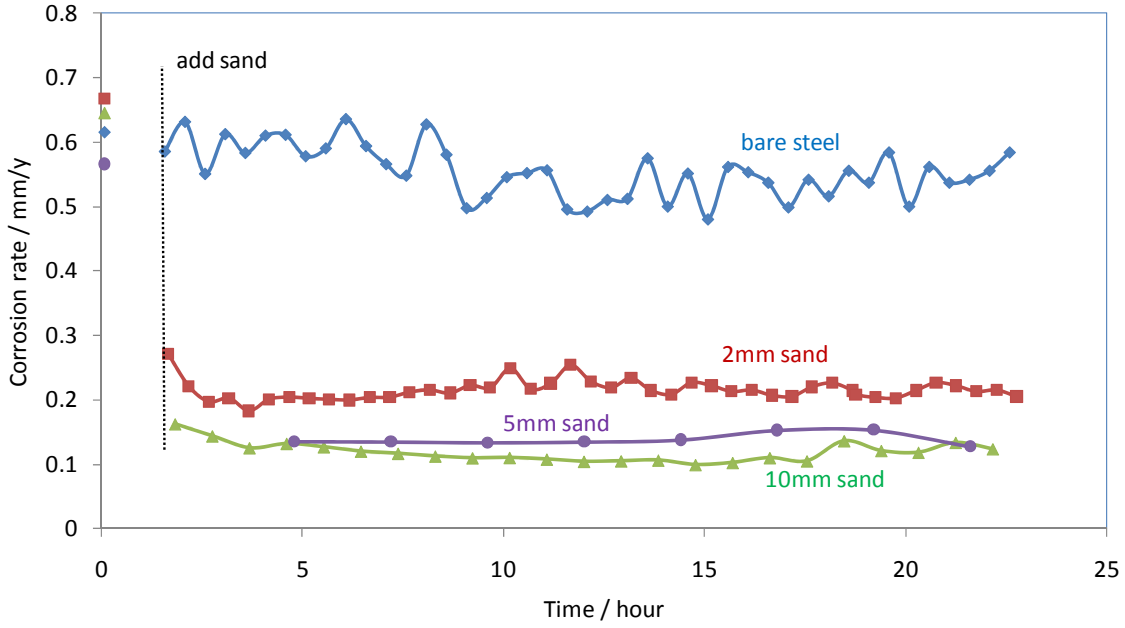

Figure 8 Comparison of CO_2 corrosion rate for mild steel in the presence of sand deposit of different thickness at pH 5 and 25°C.

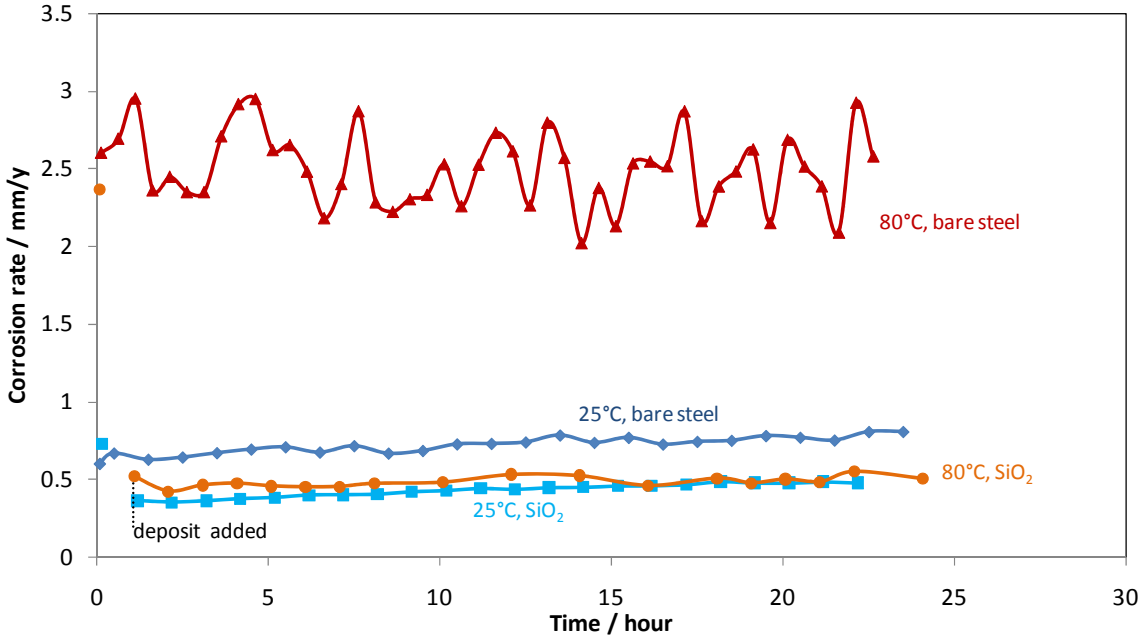

Figure 9 Comparison of CO_2 corrosion rate of bare steel and steels with 5mm SiO_2 deposit at pH 5 and different temperatures.

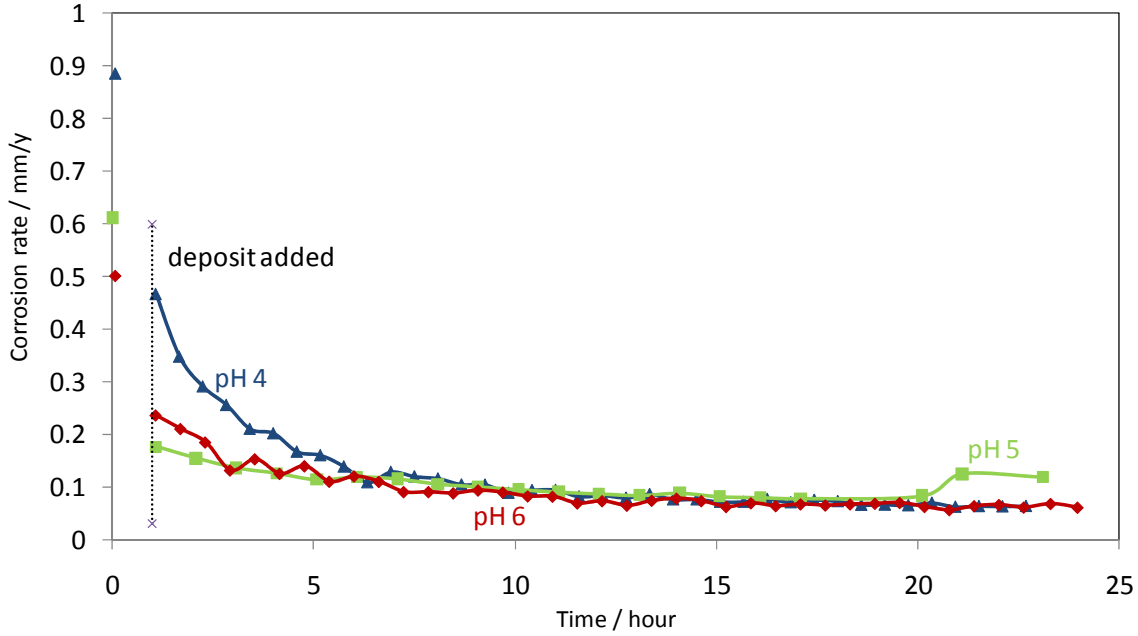

Figure 10 Comparison of general CO_2 corrosion rate between bare steel and steel with sand deposit at 25°C at different bulk solution pH.

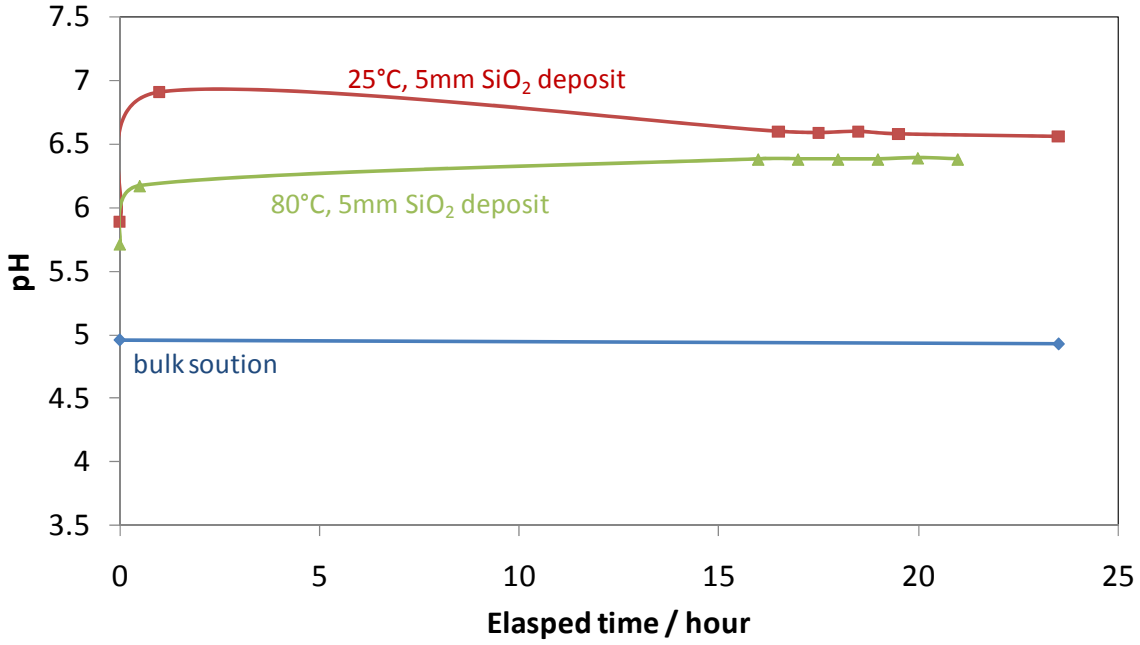

Figure 11 Comparison of pH underneath a SiO_2 powder deposit on mild steel corroding in CO_2 solution ; bulk solution at pH 5.

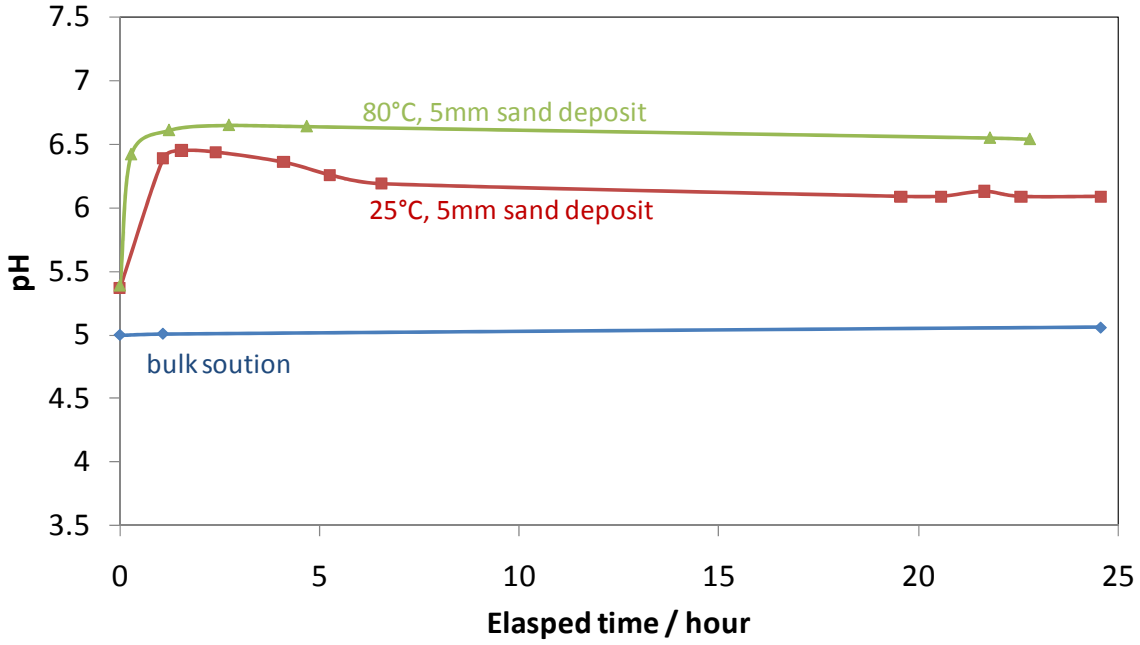

Figure 12 Comparison of pH underneath a sand deposit on mild steel corroding in a CO_2 solution ; bulk solution at pH5.

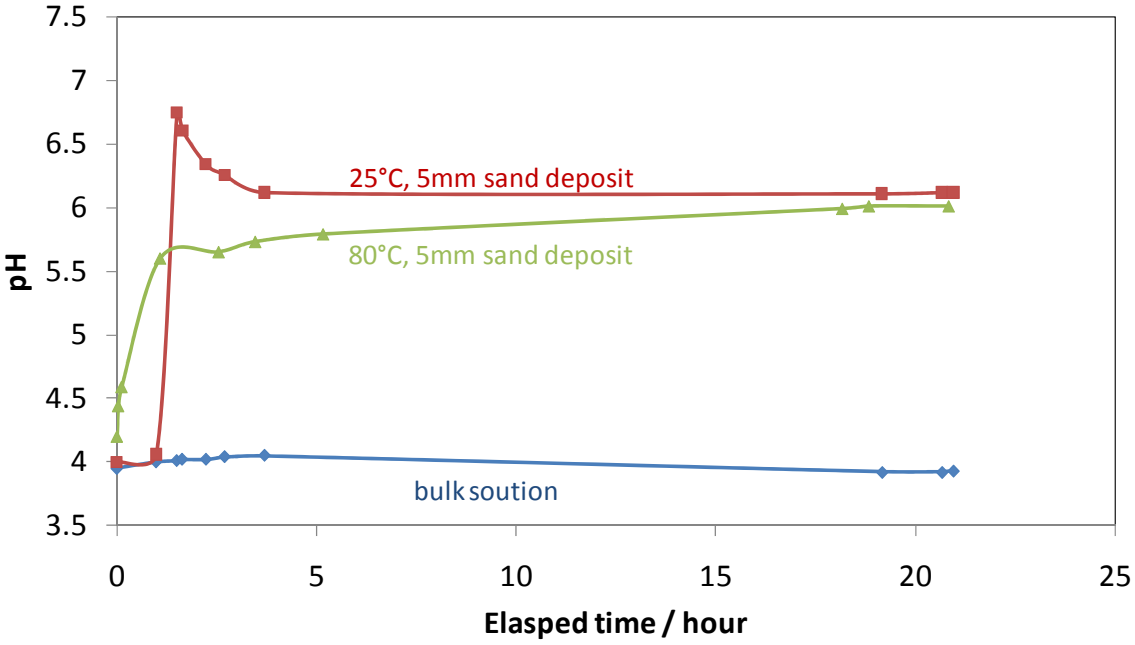

Figure 13 Comparison of pH underneath a sand deposit on mild steel corroding in a CO_2 solution; bulk solution at pH5.

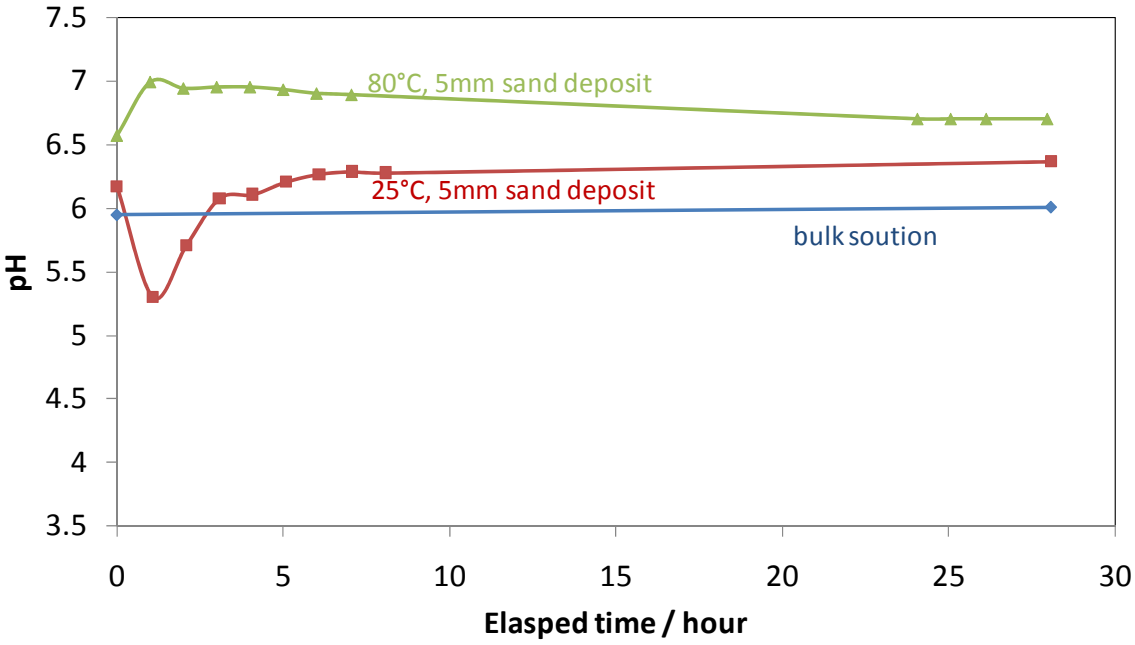

Figure 14 Comparison of pH underneath a sand deposit on mild steel corroding in a CO_2 solution; bulk solution at pH6

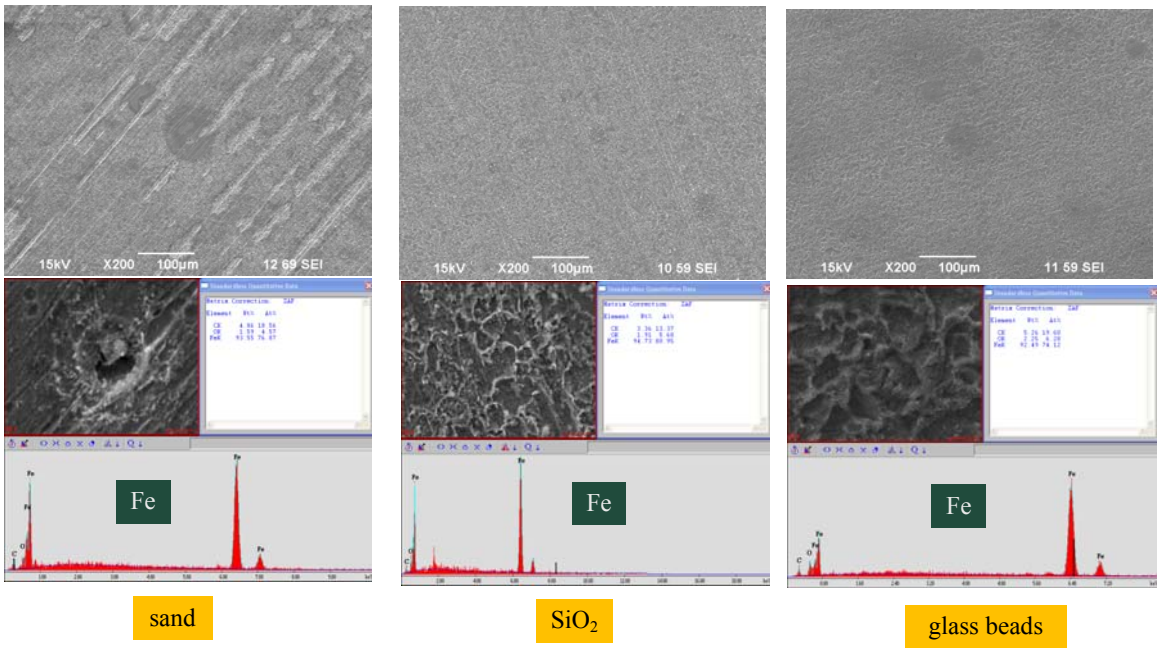

Figure 15 SEM and EDX images for mild steel surface corroded underneath various deposit layers for 24 hours at bulk solution pH 5 at 25°C.

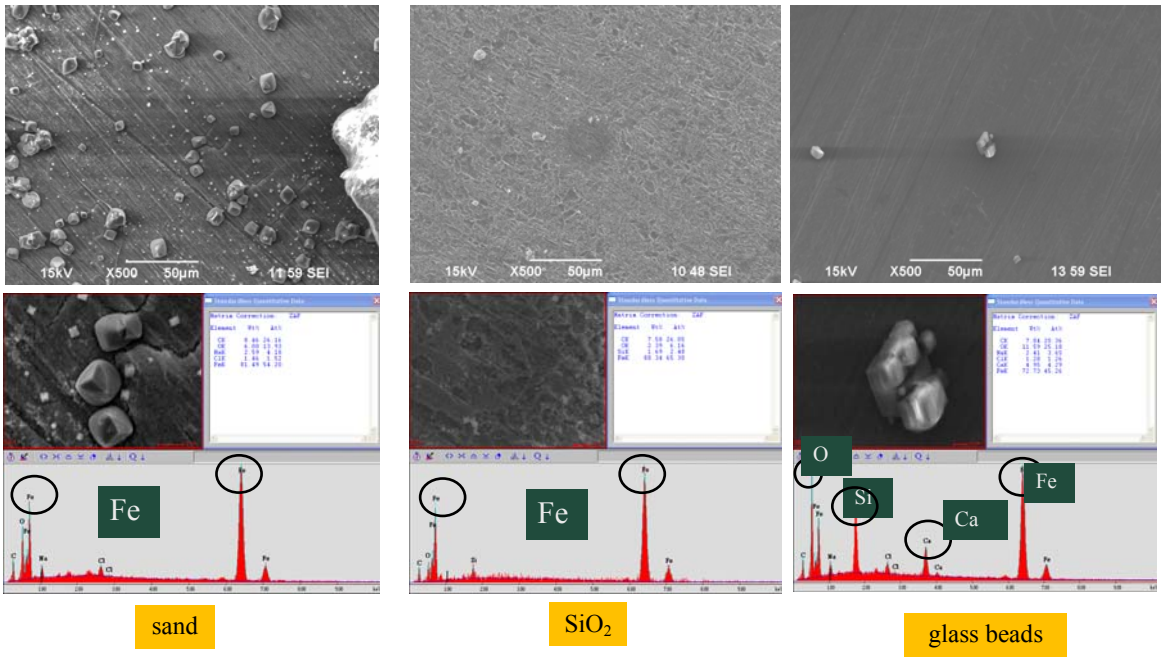

Figure 16 SEM and EDX images of mild steel surfaces corroded underneath various deposit layers for 24 hours at bulk solution pH5 at 80°C.

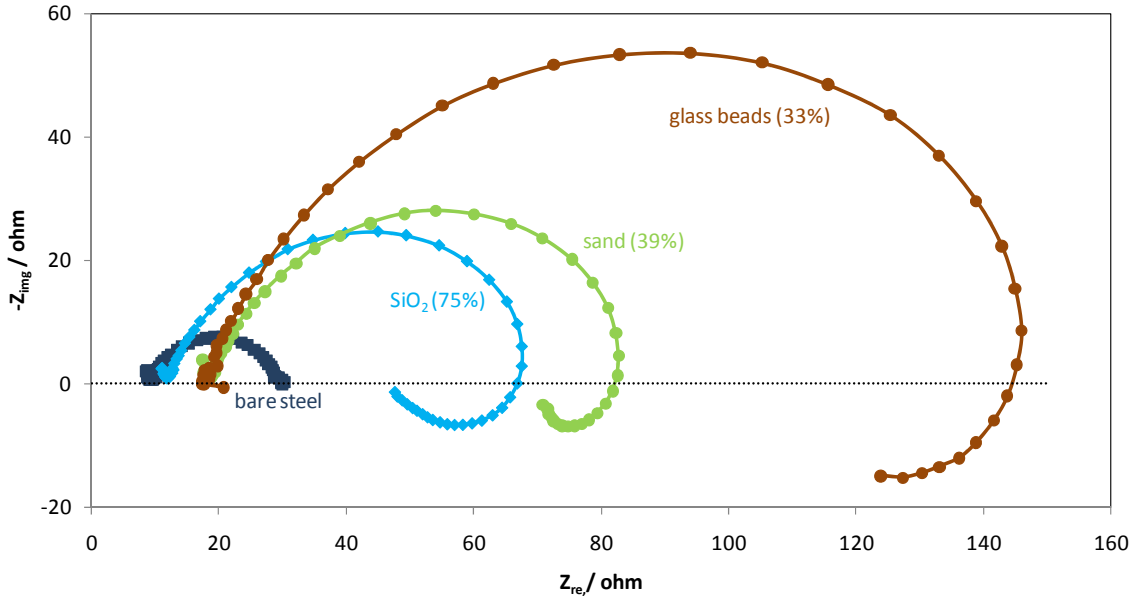

Figure 17 Nyquist curves: impedance plane displays of mild steel in CO_2 corrosion with and without the 5mm deposits at pH 5 and 25°C.

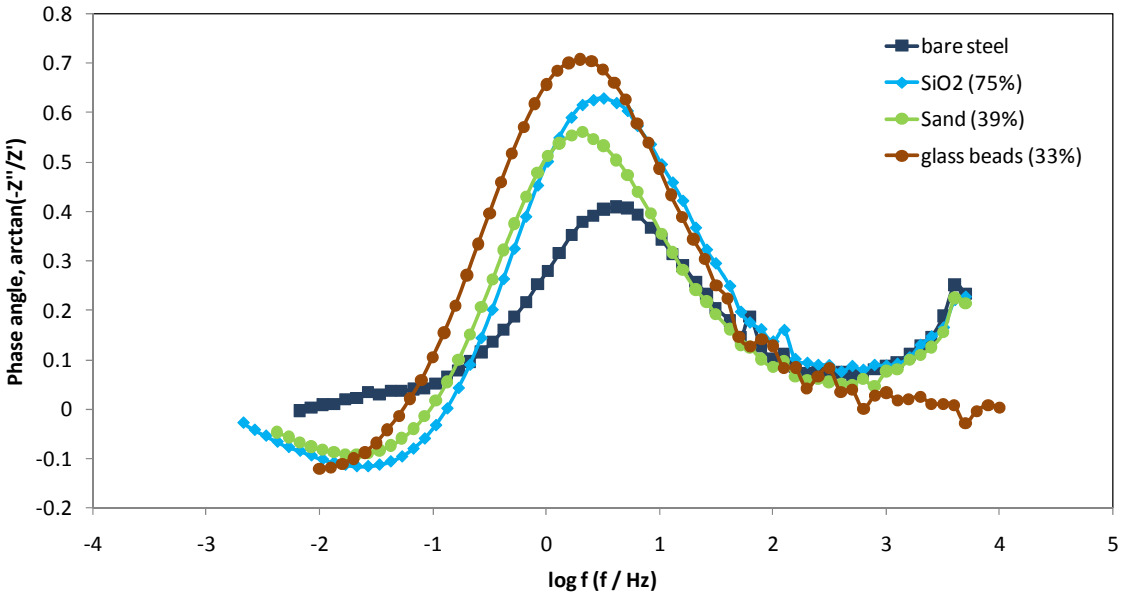

Figure 18 Bode plots for CO_2 corrosion of mild steel with and without a 5mm deposits at pH 5 and 25°C.

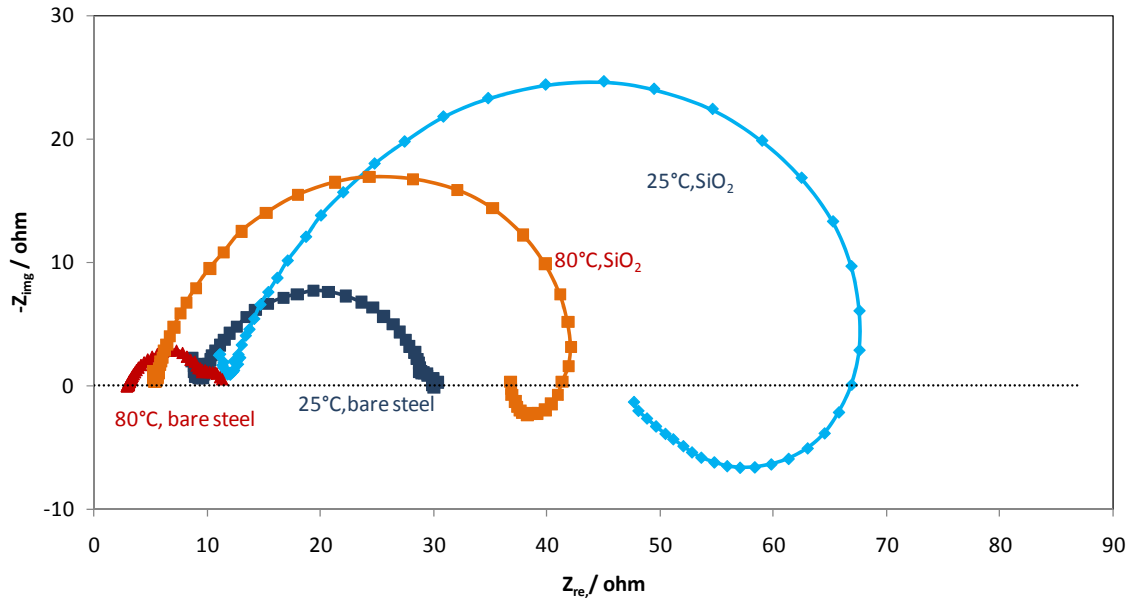

Figure 19 Nyquist curves for CO_2 corrosion of mild steel with and without a 5mm SiO_2 deposit at pH 5 at different temperatures

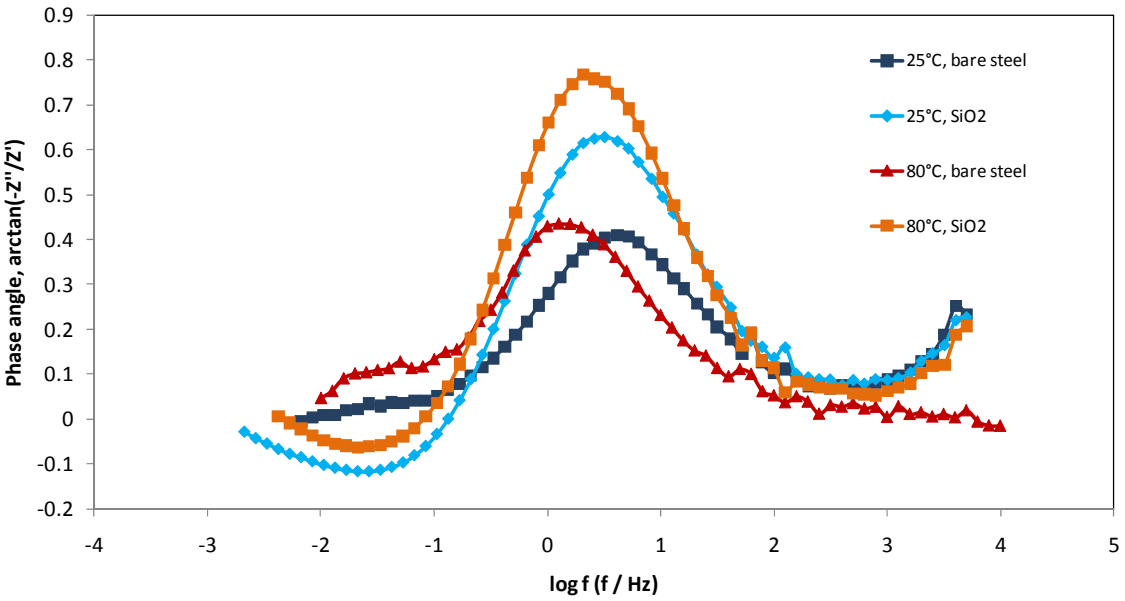

Figure 20 Bode plots for CO_2 corrosion of mild steel with and without 5mm SiO_2 deposit at pH 5 at different temperatures